Performance of WRF Large-Eddy Simulations in summertime CBL characteristics over the Taklimakan Desert: A Real Test Case

Hongxiong Xu[1], Yinjun Wang[1], Minzhong Wang[12] Wenyue Cai[13]

1 State Key Laboratory of Severe Weather, Chinese Academy of Meteorological Sciences
Beijing, China 100081

2 Institute of Desert Meteorology, CMA (Chinese Meteorological Administration),
Urumqi, China

3National Climate Center, Chinese Meteorological Administration,
Beijing, China 100081

Submitted to ***Journal of Meteorological Research***

January 2, 2018

Corresponding author:
Dr. Yinjun Wang
State Key Laboratory of Severe Weather
Chinese Academy of Meteorological Sciences
No. 46, Zhongguancun South Street, Haidian District, Beijing
P. R. China, 100081
Email: dorn1984@163.com

Abstract

During the summer season over Taklimakan Desert, the maximum height of the CBL (convective boundary layer) can exceed 5,000 m, which appeared to play critical roles in simulating the regional circulation and weather. In this paper, we use a combination of WRF-LES (Weather Research and Forecasting Model Large-Eddy Simulation) and the GPS radiosonde and eddy-covariance station to evaluate the performance of WRF-LES in the deep convective PBL case over the central Taklimakan. Results show that the model reproduces reasonably well the evolution of PBL processes. However, simulations are relative warmer and moister than those observed due to the over-predicted surface fluxes and largescale advection. Tests are further performed with multiple configurations and sensitive experiments. Sensitivity tests to Lateral Boundary Condition(LBC) showed that the model results are sensitive to changes in time resolution and domain size of Specified LBC. It is found that larger domain size varies the distance of the area of interest from the LBC, is efficient to reduce the influences of large forecast error near the LBC. However, the more frequently updated LBC is desirable to inhibit model error near the LBC. Forecast error increased as the distance between the area of interest and the lateral boundaries decreased. Furthermore, comparing model results using the original surface land parameterized sensible heat(SH) with those of sensitive experiment, it is concluded that a reduction(increment) in SH decreases(increases) maximum PBL by roughly 15% over desert. It is very sensitivity to SH produced by surface land scheme in the CBL during summer day time.

Keyword: WRF, Large Eddy Simulation, Convective Boundary Layer, Taklimakan

Introduction

The Taklimakan Desert, locates at the south center of the province of Xinjiang, China, is the world's second-largest flow desert and has profound influences on the regional weather and climate. Because of the extreme near-surface temperatures, the Taklimakan ABL commonly reaches 4–6 km during boreal summer, making it probably the deepest on earth. The deep PBL, which is significantly higher than that of the surrounding mountains and oases, appeared to play important roles on regional circulation and weather. In the northwest of china, the ability to accurately forecast in Taklimakan Desert especially the PBL processes is an important problem.

The large desert (such as Sahara, Taklimakan et al.) atmosphere is always a key component of the climate system. The surface heating from intense solar radiation leads to the development of a near-surface thermal low pressure system, commonly referred to as the heat low(Engelstaedter et al. 2015). However, despite of the vital role of the desert playing in the climate system, observations are extremely sparse and thin data that exist are mostly from the surrounding of the desert due to conditions are very difficult(Marsham et al. 2011). This fundamentally restrict the development of understanding desert and surrounding area, and leads to large discrepancies to analyses and significant biases in operational numerical weather prediction (NWP) models, given the scarcity of observation being assimilated by operational systems. The ability of these local models to simulate real-world cases is often hindered by a lack of favorable data needed to assess the performance of model results(Garcia-Carreras et al. 2015). To fill in the gaps of Taklimakan desert，the field observation experiment was held during the month of July 2016 in Tazhong, which is located at center of Taklimagan, by the Institute of Desert Meteorology (IDM), Chinese

Meteorological Administration (CMA), Urumqi(Liu et al. 2012; WANG et al. 2016a; Wang et al. 2016b). This will also give the opportunity to evaluate the performance of the deep PBL process in NWP models over Taklimakan.

On the other hand, atmospheric motions interweave small-scale, complex and multiscale nonlinear interactions. Due to the limited resolution (time and space) mesoscale atmospheric models are still cannot explicitly represent all these processes(Talbot et al. 2012). Such processes include turbulent motions, which are too small-scale to be explicitly resolved in the atmospheric model by a simplified process. Furthermore, turbulent mixing throughout the planetary boundary layer (PBL) can heavily impacted NWP forecasting (Shin; Hong 2011; Shin; Hong 2015).

One way to tackle complex turbulent flows in weather forecast models is Large eddy simulation (LES) which explicitly resolve energy-containing turbulent motions that are responsible for most of the turbulent transport(Moeng et al. 2007). It has been used intensively to examine detailed turbulence structure, to generate statistics, and to perform physical-process studies(Garcia-Carreras et al. 2015; Heinold et al. 2013; Heinold et al. 2015; Heinze et al. 2015; Sun; Xu 2009). However, most LES applications to the PBL have been limited to idealized physical conditions. Recently, some studies attempt to test LES and assess its performance in simulating real cases(Liu et al. 2011; Talbot et al. 2012). Liu et al. (2011) suggests that WRF-LES is a valuable tool for simulating real world microscale weather flows and for development of future real-time forecasting system, although further LES modeling tests, such as elucidate whether inaccurate synoptic forcing or coarse resolution, are highly recommended. Talbot et al. (2012) suggested that the ability of WRF-LES to simulate real-world cases are hindered by a lack of favorable synoptic forcing. The initial and lateral boundary conditions was found to be more critical to the LES results than subgrid-scale turbulence closures. Thus, the initial condition of can significantly alter high-resolution LES status through WRF land-surface model.

However, most of research above on LES over desert has been limited to idealized physical conditions(Garcia-Carreras et al. 2015) or conducted real case outside Taklimakan(Liu et al. 2011; Talbot et al. 2012). As far as we know, this study is the first attempt to applicate LES in real case over Taklimakan. Thus, an important aspect of the ongoing this paper is to examine assess the skillfulness of WRF-LES in relative coarse resolution (333m) over Taklimakan dessert, in simulating real cases of desert PBL process during boreal summer events in Taklimakan. First we assess the potential errors related to LBC. Then we use a combination of WRF-LES and the GPS radiosonde and surface fluxes calculated by an eddy-covariance method taken in the central Taklimakan to evaluate the performance of WRF-LES in real case. Moreover, we aim to evaluate the relative contribution of uncertainties in surface model to the typical behavior of PBL processes by conducting the sensitivity experiments. Thus, the sensitivity of the performance to surface sensible heat flux (SH) is also studied. Section 2 gives a brief description of synoptic of the study case. In Section 3, we described data and model configuration and design of numerical experiments used in this study. We presented the results of numerical simulations in Section 4. Finally, we summarize conclusions in Section 5.

1 Synoptic

Figure 2 shows the synoptic patterns at 0800 BJT 1 July 2016 at 850 700 500 and 100 hPa. There were cyclonic vortex from 850 to 500 hPa center at 55° N (Figure 2a ,b and c). Taklimakan was located east of cyclonic vortex and embedded in east–west-elongated ridge at 0800 BJT 1 July. To the southwest, influenced by the South Asia High, which was centered over the eastern Iranian Plateau, the upper air over the Taklimakan Desert was controlled by the westerly jet stream at 100hPa (Figure 2 d). The high-pressure system at low level, which is termed of heat low (Figure 3), dominated most of southern Xinjiang and resulted in continuous high temperature over the desert. This situation favored the subsidence motion and served as a triggering mechanism for deep PBL in the region in the coming 2–3 days (not show).

2 Method

2.1 Data

In this study, model simulations compared for 12 hours from the Tazhong field experiment, from 0800 BJT 01 July to 2000 BJT 01 July 2016. The field observation experiment was held during the month of July 2016 in Tazhong, by the Institute of Desert Meteorology (IDM), Chinese Meteorological Administration (CMA), Urumqi. The main station was located at 86.63° E, 39.03° N. The location is relatively flat with few hills and covered by sand combined with grass (Figure 1), and the 12-h period of our simulation was under a cloudless sky and dry environment. We conducted one way nest WRF from mesoscale(12km) down to LES-scales(0.33km) and compare its results to various instruments including:

1) surface fluxes: The eddy correlation system was a R3-50 supersonic anemometer

developed by Gill Company, UK, deployed at a height of 10 m. The data acquisition frequency was 20 Hz, and the surface sensible heat flux was calculated by the eddy-covariance method.

2) vertical profiles measured using soundings: Upper air soundings of temperature, pressure, humidity, and wind speed and direction were conducted 3-6 times per day with the GPS sounding system developed by No. 23 Institute of China Aerospace Science & Industry Corp. (CASIC23). The sounding times were 01:15, 07:15, 10:15, 13:15, 16:15 and 19:15 respectively.

2.2 Model configuration

The WRF model of version 3.8.1 (Skamarock et al. 2008) is utilized here at convection-permitting resolutions to simulate the extreme rainfall event. The model is integrated for 12h, starting from 0800 BJT 01 Jul 2016. Figure 1 shows the domain for two experiments. We use the outermost domain and three one-way nested domains. The model horizontal spacing is 12km 3km 1km and 0.33km for d01 d02 d03 and d04. The sizes of model grids are 411 ×321 791x651 211x201 and 403x406 respectively (Figure 1). All domains were 51 levels extended to 50 hPa.

The initialized condition and lateral boundary conditions are provided to the coarsest mesoscale simulations from NCEP Global Data Assimilation System (GDAS) Final Operational Global Analyses. The analyses are on 0.25-degree by 0.25-degree grids prepared operationally every six hours and available on the surface, at 26 mandatory (and other pressure) levels from 1000 millibars to 10 millibars(National Centers for Environmental Prediction 2015).

The model physical options include the WSM5 microphysics scheme(Hong; Lim 2006), the Yonsei University (YSU) planetary boundary layer scheme (Hong; Pan 1996), the Kain–Fritsch cumulus parameterization scheme(Kain 1993; Kain 2004), the Noah land surface model(Chen; Dudhia 2001a, 2001b), the Rapid Radiative Transfer Model(Mlawer et al. 1997) longwave, and the Dudhia shortwave radiation scheme (Dudhia 1989). The cumulus parameterization scheme is only applied to the d01(12km) grid domain to parameterize the convective rainfall. While, the large-eddy-simulation (LES) is only applied to d04(0.333km).

3 Results

3.1 Sensitive to Lateral Boundary Condition(LBC)

Before moving on to the details of the LES simulations, we first assess the sensitivity of the LES simulations to time resolution and domain size of Specified LBC. For one-way nest, Specified LBC obtained from coarser model simulation. The analysis and all forecast times from a previously-run larger-area model simulation are used to specify the LBC. The primary cause of differences in PBL structure was diagnosed as differences in domain size and frequency provided by the coarser resolution. The aim is to assess the sensitivity of the finer large-eddy simulations to time frequency and domain size of Specified LBC forcing by larger-area model simulation; the details of the three simulations are given in Table 1.

Figure 4 and Figure 5 compare the profiles of the simulated potential temperature and vapor mixing ratio profiles from LBC sensitivity experiments and observation. Results indicate that, there is a distinct relationship between LBC and CBL development. All model-produced profiles are nearly the same at initial time (not show). However, the comparison results reveal that discrepancies from different experiments are large for CBL.

The results indicate that, with larger domain size and more time frequency LBC leads to a warmer and drier lower PBL and a cooler and moister free troposphere. Such sensitivity is monotonic with respect to LBC (Figure 4 and Figure 5). Furthermore, the potential temperature profiles within CBL become divergence at 1100 BJT. In the next three hours, the differences between the sensitive experiments keep increasing with time (Figure 4 a, b). However, the results show more convergence at afternoon as CBL continues to grow (Figure 4 c). Finally, largest discrepancies are found by end of the day (Figure 4 d) where the model CBL potential temperature is warmer by up to about 0.7K and 0.9K in BDY_T2 and BDY_T1 respectively, compared to measurements.

The more frequently updated LBC is desirable to cold zone near the LBC, which results in cold advection of the temperature and moisture to the area of interest (Figure 7 b, c). Larger domain size, which varies the distance of the area of interest from the LBC, is efficient to reduce the influences of large forecast error near the LBC to the area of interest (CMP Figure 7 a, c). The results suggest that the model results are sensitive to changes in time resolution and domain size of Specified LBC. The mismatch among sensitive experiments is present means that the effect of LBC needs to be quantified to realize a more realistic performance. Extra care should also be taken with domain size and frequency of LBC.

3.2 Validation of the deep CBL structure

Simulated diurnal surface variables at Tazhong station from CTRL simulation for 01 July 2016 are presented in Figure 6 a, b. Results show that discrepancies of thermodynamic surface variables (the surface temperature, sensible and latent fluxes) between model and observation are large during simulation. The SH is far less in observation (maximum: 243 W

m^{-2}) relative to model (maximum: 613 W m^{-2}). This represents SH from WRF simulation is 2.5 times than that of observation when both of which reach its maximum. On the other hand, model shows a significant cold bias for the surface temperature. The surface temperature is much higher in observation (maximum: 70 °C) relative to model (maximum: 50 °C).

Three possible reasons result in model SH far above that of observation: （1） the mismatch of land-use between the model and the observation. WRF use land-use categories to assign certain static parameters and initial values to each grid cell, for example, albedo, surface roughness, and so on(Schicker et al. 2016). (2) it is should be noted that the SH and LH based on eddy correlation might be underestimated. Researchers found that if the other two terms in the budget—net radiation and flux into the soil were accurate, used data for the whole experiment to find the H + LE for Tazhong station are equal to an average of 70% of what would be required for balancing the surface energy budget(LeMone et al. 2013).

Despite the large surface differences, near-surface variables (2m temperature, relative humidity and 10m wind speed) are closer to measurements than at surface, but their values are relatively higher than those observed (Figure 6 e). The time series evolution of 2m temperatures nearly follow those of the observations; but model produce warmer surfaces by about 3 K at the beginning of model integration, and 1K when model and observation both reach their maximum temperature, respectively.

Results indicate that, model-produced near-surface relative humidity is close to observations at initial time (Figure 6 f). However, the humidity from the model keeps increasing at the first few hours of model integration, when observations decrease. After 3 hours' spin-up, the model reproduces reasonably well the evolution of humidity, in agreement with observation, but their values are relative higher than those observed.

One reason for this discrepancy is the overestimate of soil moisture during simulation. Soil moisture can severely impact near-surface humidity. The overestimate of the soil moisture contents in the initial condition of the model, which are only offered to the model at the first-time step, may result in considerable differences in near-surface layer humidity. (Talbot et al. 2012). In the present simulations, model results are reported to produce grossly overestimate soil moisture. At the model initialization for the CTRL simulation, EC station at Tazhong station indicated a value of the 5-cm-deep soil moisture of 0.230 m^3/m^3, while the model initial value is 0.6 m^3/m^3 (Figure 6 d). This large overestimate of soil moisture results in LH (Figure 6 b, f) from the model to continue increasing, then forces near-surface far moister than observation at the first few hours of model integration. An interesting result to note is that the model simulation has the abilities to correct some of the bias due to the initial condition of the surface; the results from CTRL experiment are closer to observation after 3 hours' spin-up.

The model simulated potential temperature are compared to GPS sounding measurements at Tazhong during 0800~2000 BJT 01JULY2016 in Figure 4. At 0800 BJT, when the model is initialized, the nocturnal inversion reaches 300m (not shown). By 1100 BJT, this inversion is eroded in the model in agreement with observations, and both reaching about 300m at 1100 BJT. However, the simulated CBL grows faster in the morning due to larger SH than observation, reaching 3500m (3000m in the observations) at 1400 BJT, At 1700 BJT, the simulated and observed CBL heights exceed 4000m and 5000m respectively.

This indicates that the simulated CBL grows more slowly in the afternoon than measurement. Compared to measurements, the model is initially cooler with faster heating in the morning. As a result, model is warmer than measurements in the afternoon. Eventually, model agrees with observations at the end of the day. The main source of model error is inauthentic cold advection within PBL in the afternoon which will be discussed below. Another possible minor reason is the differences of potential temperature lapse rate above the top of mixing layer between observation and simulation, simulated stronger inversion layer restrain the development of CBL.

Moreover, in terms of CBL temperatures, the model initially simulates a cooler and drier PBL than that observed, at 1100 BJT01 JUL (Figure 4a). Compared to the observed potential temperature profile, the CBL seems to appear earlier in model forecasts result based on obvious warming in surface layer. However, when the SH has reached its maximum extent at 1400 BJT (Figure 4b), potential temperature profile is closer to measurements than at initial time, and their values are higher than those observed. By 2000 BJT (Figure 4d), PBL height in the model reaches its maximum value, consistent with observation, although approximately 0.4K cooler on the lower levels(<2.5Km). As mentioned, one cause of the higher temperatures produced with model would be the large difference in the surface heat fluxes. it was concluded that the surface sensible heat flux from the land surface parameterization is the crucial factor affecting the CBL process during summer day time. Differences in surface SH would create differences in the vertical development of the PBL. Thus, the large surface SH difference between the model and observation may lead to differences in CBL growth during daytime and in its peak depth during the simulation. Fortunately, one can artificially modify the surface SH computed by surface-land model, which controls the calculation of surface fluxes. Sensitive simulations will be realized and discussed in section 6.

Figure 5 shows Vertical profiles of vapor mixing ratio at Tazhong station. The simulated profiles with lower RL are much drier than observation from 1500 to 3500m at 1100 BJT. The vertical mixing results in the uniform structure of vapor mixing ratio within CBL, so the differences between simulated and observational profiles are reduced remarkably when CBL reach above 4000m at 1400 BJT. Differences are generally less than 1g/Kg at 1100 BJT reaching a maximum of 0.3g/Kg at 1400 BJT. However, measured PBL moisture shows an inverse layer at lower PBL(≤2000m) range from 2.8 to 3.6 g/Kg, which is not captured by model. Furthermore, as the convective boundary layer grows, the inversion moisture structure below 3000m develops to and maintains below 3000m during 1400~2000 BJT. By the end of the day, the model-simulated CBL humidity show moister than observation with no inverse moisture layer within CBL, which is quite different from observation.

Inverse humidity may be caused by the joint of the heterogeneous humidity Pattern and Large-scale advection over the underlying surface. For instance, interaction of oasis with desert environment may resulted in the inverse humidity layer in desert PBL. Thus, one possible reason for the discrepancy between model and observation caused by the error in land-use. The USGS land-use in ARW-WRF is based on AVHRR (Advanced Very High Resolution Radiometer) 1km resolution satellite data during1992-1993. For our case, this land-use data may be outdated in Taklimakan. Besides such changes, misclassifications are found in the USGS land-use data, the default land-use dataset in WRF(Schicker et al. 2016).

This is also confirmed by the discrepancies of land-use between simulation and measured at the Tazhong station in the previous figure. Large-scale advection of dry air can affect the profile of moisture. Moisture will also be variable in the horizontal, so advection at the low level could contribute to the dry at bottom and moisture at the upper of PBL between 1100 and 2000 BJT at the bottom of the PBL.

The mismatch between the model and the observations in terms of moisture that is present means that the effect of land-use and Large-scale advection needs to be quantified and that more detailed data of Taklimakan (land and atmosphere) might be necessary to realize a more realistic performance. Extra care should also be taken with sparse and the limited data in the periphery of the Taklimakan(ter Maat et al. 2012).

3.3 Simulations with different surface sensible heat(SH)

The primary cause of differences in PBL structure was diagnosed above as differences in surface sensible heat flux predicted by the surface-land schemes. The surface sensible heat flux is the dominant factor affecting the CBL depth during summer day time. Thus, this difference between the model and observation may lead to differences in PBL growth during daytime and in its peak depth during the simulated day; To further confirm whether this indeed occurs, two additional sensitive simulations were realized based on the CTRL experiment. For HFX-125% HFX -75% the surface sensible heat flux is %125 and %75 that of CTRL（HFX -100%） experiment, while the other parameters remain the same.

The results indicate that, with smaller SH leads to a cooler and moister lower PBL and a warmer and drier free troposphere. Such sensitivity is monotonic with respect to SH. Overall, the CBL structure determined from the HFX-%75 matches the GPS measurements better than the CTRL（HFX-100%）simulations. Potential temperature profiles from CTRL（HFX-100%）CTRL（HFX-125%）are consistently warmer than the observation by about 0.4 and 0.5 K respectively, while results from CTRL（HFX-100%）are within about 0.2K at 1400 BJT. Simulation results converge at the end of the day, but remain differences at 2000 BJT. The results suggest that the model results are sensitive to changes SH from land-surface model.

4 Summary

This paper assesses the performance of the Weather Research and Forecasting Model (WRF) Large-Eddy Simulations(LES) in deep convective PBL case over Taklimakan Desert. Tests are performed with multiple configurations and sensitive experiments. Sensitivity tests to Lateral Boundary Condition(LBC) showed that the model results are sensitive to changes in time resolution and domain size of Specified LBC. It is found that larger domain size varies the distance of the area of interest from the LBC, is efficient to reduce the influences of large forecast error near the LBC. Whereas, the more frequently updated LBC is desirable to inhibit model error near the LBC. Air variables (air temperature, relative humidity and 10m wind speed) are closer to measurements than at surface, but their values are relative higher than those observed. However, it is found that discrepancies of thermodynamic surface variables (the surface temperature, sensible and latent fluxes) between model and observation are large during 12h simulation.

Consequently, with the configuration used in this study, the model reproduces reasonably well the evolution of PBL processes. The model shows discrepancies between the main CBL characteristics in the morning including the thermal and moisture structure. The model simulates the relatively colder and drier morning CBL well, underestimating it by up to

1.5K near-surface layer at Tazhong station. In the case of the underestimation of moisture by only up to 1 g/kg in the near-surface layer. the overestimation of CBL profile may be caused by discrepancy between model and measurement initially. This indicates that the results are sensitive to the model initial conditions. An interesting result to note is that the model simulation seems to be able to correct some of the bias due to the initial condition. In the afternoon, the model struggles to correctly simulate the thermal structure, but simulations are relative warmer and moister than those observed. Theta profile which at CBL appears warmer by up to about 0.4K compared to the observations. While the model overestimate the afternoon moisture seriously, it mainly overestimates vapor mixing ratio by about 1 to 2 g/Kg in the CBL. Largest discrepancies are found in 0~3Km where the model vapor is twice as moist (up to about 3g/Kg above AGL) as observed.

Furthermore, two additional sensitive simulations were realized to further confirm whether large differences of SH lead to differences in ABL growth during daytime, based on the CTRL experiment. The results suggest that the model results are sensitive to changes SH from land-surface model. From these results, it was concluded the surface sensible heat flux is the dominant factor affecting the CBL depth over Taklimakan during summer day time. Thus, the large difference between the model and observation may lead to differences in CBL growth during daytime and in its peak depth during the simulation.

The future work aimed to study several other deep CBL cases over Taklimakan to summarize their common features. Furthermore, we hope to utilize high resolution model and observation to describe the fine characteristics of a typical deep Taklimakan CBL by, particularly the turbulent and vertical mixing and its impact on regional weather forecast. This research is aimed to improve the understanding of deep CBL over Taklimakan and its influence on regional weather and climate.

Conflict of Interests

The author declares that there is no con ict of interests regarding the publication of this paper.

Acknowledgments

This study is supported by the State Key Program of National Natural Science Foundation of China (Grant no. 41575008). The author would like to thank all the reviewers and editors for their professional advice to improve the paper.

Captions:

Figure 1 Simulation domains used in ARW model with terrain height (shaded, units:m); (b) land use categories for domain D03 and D04

Figure 2 Horizontal distribution of geopotential height (solid, units: dagpm), wind speed (shaded, units: knot), and wind barbs from the NCEP FNL analysis at 0800 BJT 1 Jul 2016 at (a) 850 hPa, (c) 700 hPa, (e) 500 hPa, and (d) 100hPa.

Figure 3 NCEP fnl 700hPa potential temperature (colors) and mean sea level pressure (white lines) at 0800 BJT 1 Jul 2016. The black dot shows the location of Tazhong station at Xingjiang province.

Figure 4 Vertical profiles of potential temperature (units: K) at (a)1100 (b) 1400 (c) 1700 (d) 2000 BJT 01 Jul2016

Figure 5 The same as Figure 4, but for vapor mixing ratio (units: g/Kg)

Figure 6 Time series of simulated surface initial at 0800 BJT 01July 2016 (a) sensible heat flux (W/m2), (b) latent heat flux(W/m2), (c) 2-m temperature (◦C), (d) surface temperature (◦C), (e) 2-m Relative Humidity(%) and (f) 10-m wind speed (m/s) with corresponding observations.

Figure 7 cross sections along 39.03°N of horizontal winds (barbs, units: m/s), at intervals of 5 m/s, superposed with theta (shaded, units: K) and vapor mixing ratio(contour, units: g/Kg), from (a) BDY_T1, (c) BDY_T2, (e) BDY_T3 experiments at1400 BJT 01JUL2016, (b), (d), (f) are the same as (a), (c), (e), but for 2000 BJT 01JUL2016.

Figure 8 The same as Figure 4, but for SH flux sensitive experiment

Figure 9 The same as Figure 8, but for vapor mixing ratio (units: g/Kg)

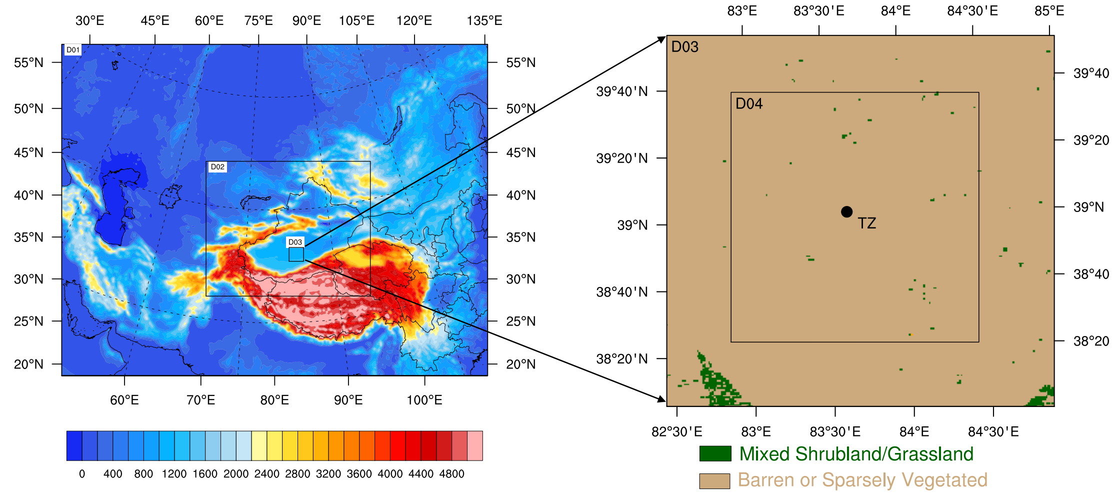

（a）　　　　　　　　（b）

（c）

Figure 1 Simulation domains used in ARW model with terrain height (shaded, units:m); (b) land use categories for domain D03 and D04; (c) photograph of Tazhong station

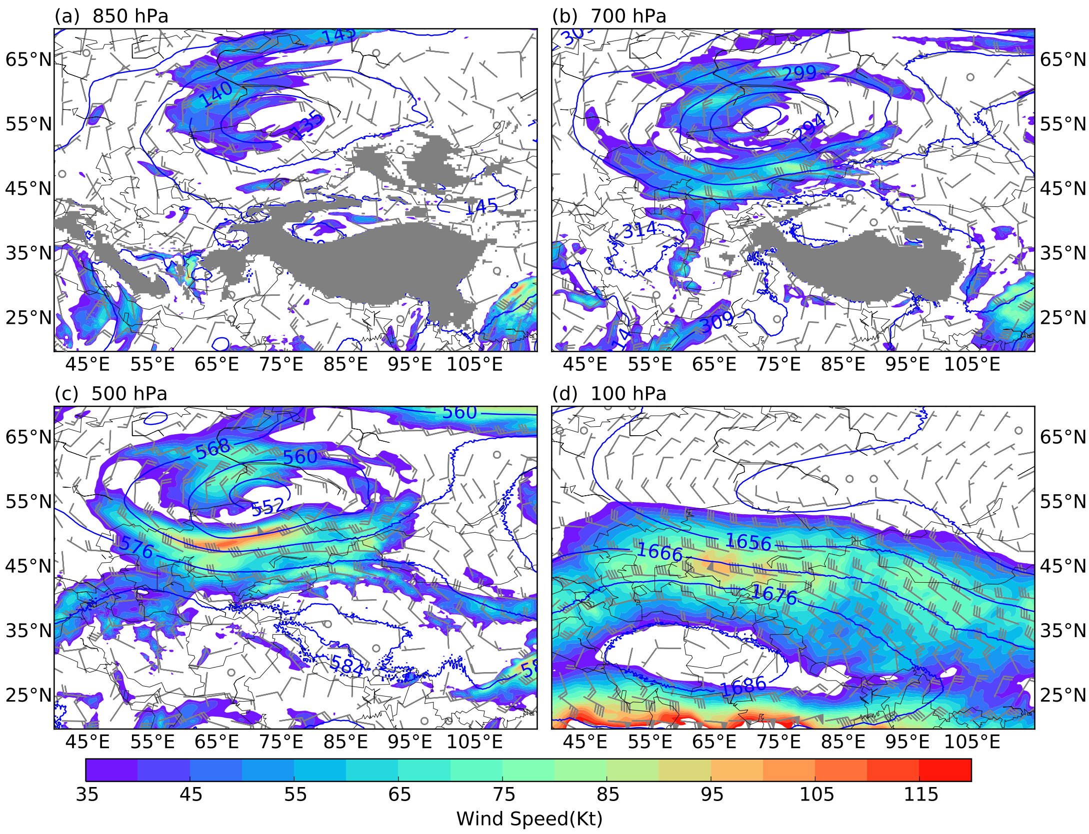

Figure 2 Horizontal distribution of geopotential height (solid, units: dagpm), wind speed (shaded, units: knot), and wind barbs from the NCEP FNL analysis at 0800 BJT 1 Jul 2016 at (a) 850 hPa, (c) 700 hPa, (e) 500 hPa, and (d) 100hPa.

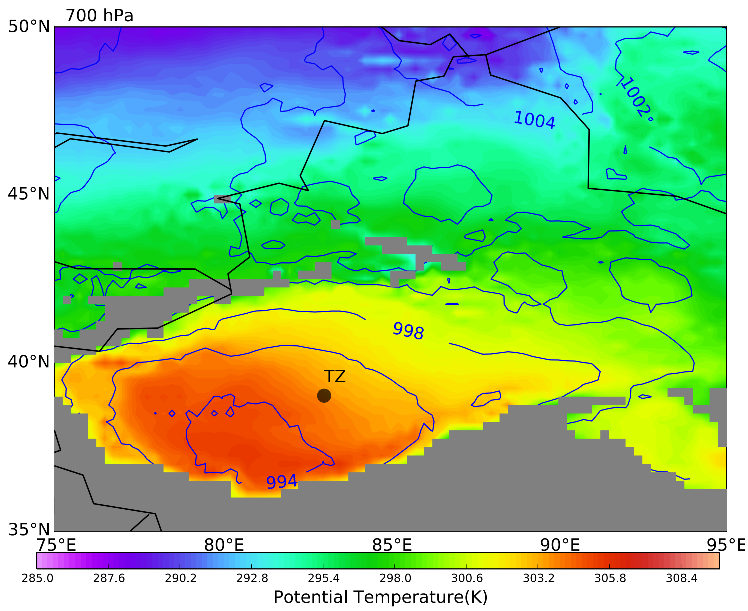

Figure 3 NCEP fnl 700hPa potential temperature (colors) and mean sea level pressure (white lines) at 0800 BJT 1 Jul 2016. The black dot shows the location of Tazhong station at Xingjiang province.

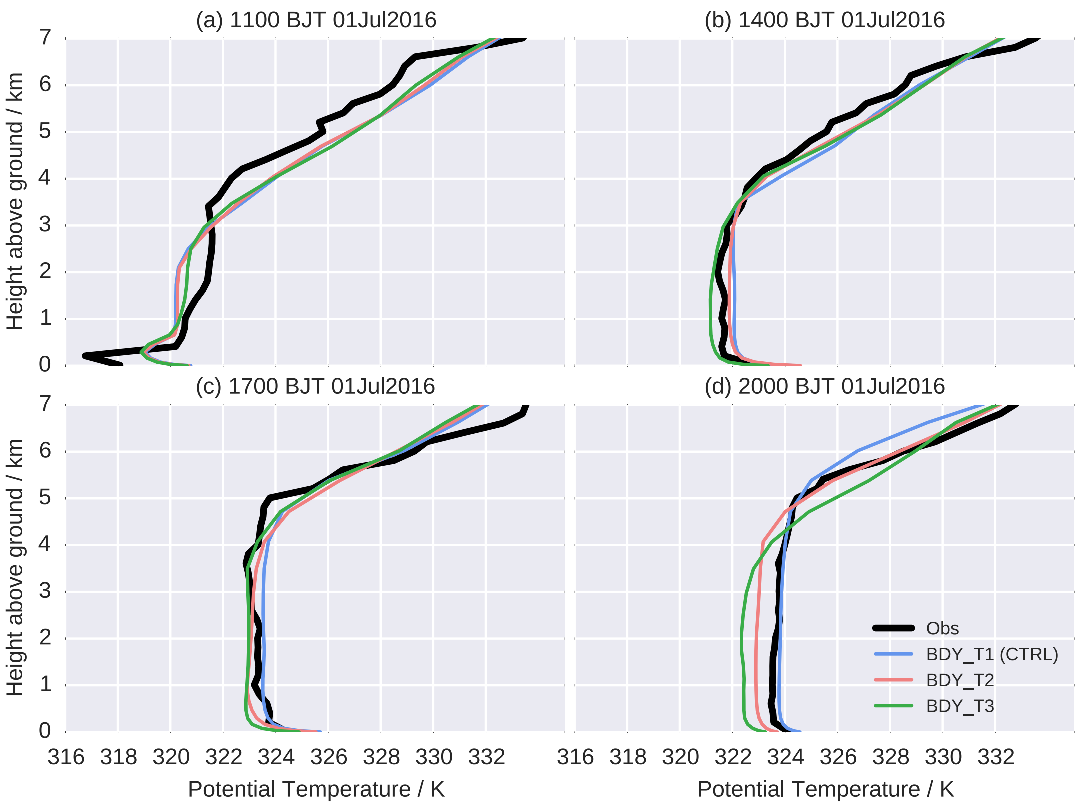

Figure 4 Vertical profiles of potential temperature (units: K) at (a)1100 (b) 1400 (c) 1700 (d) 2000 BJT 01 Jul2016

426

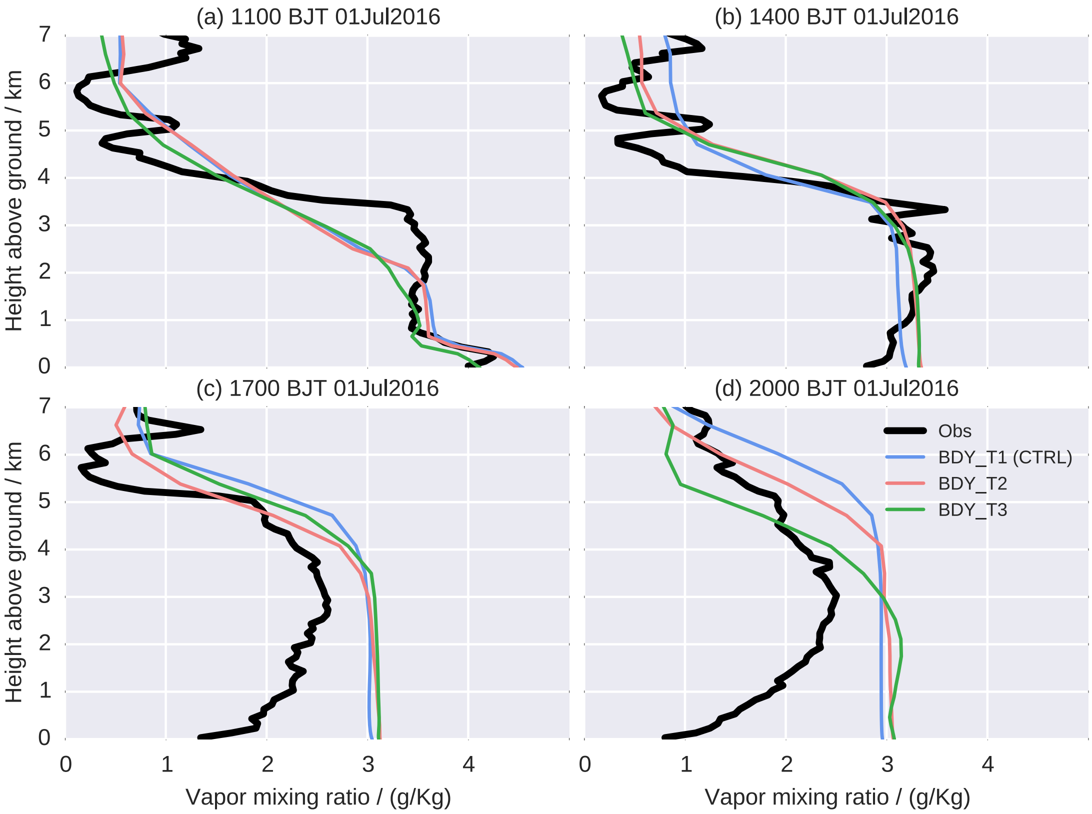

427

428 Figure 5 The same as Figure 4, but for vapor mixing ratio (units: g/Kg)

429

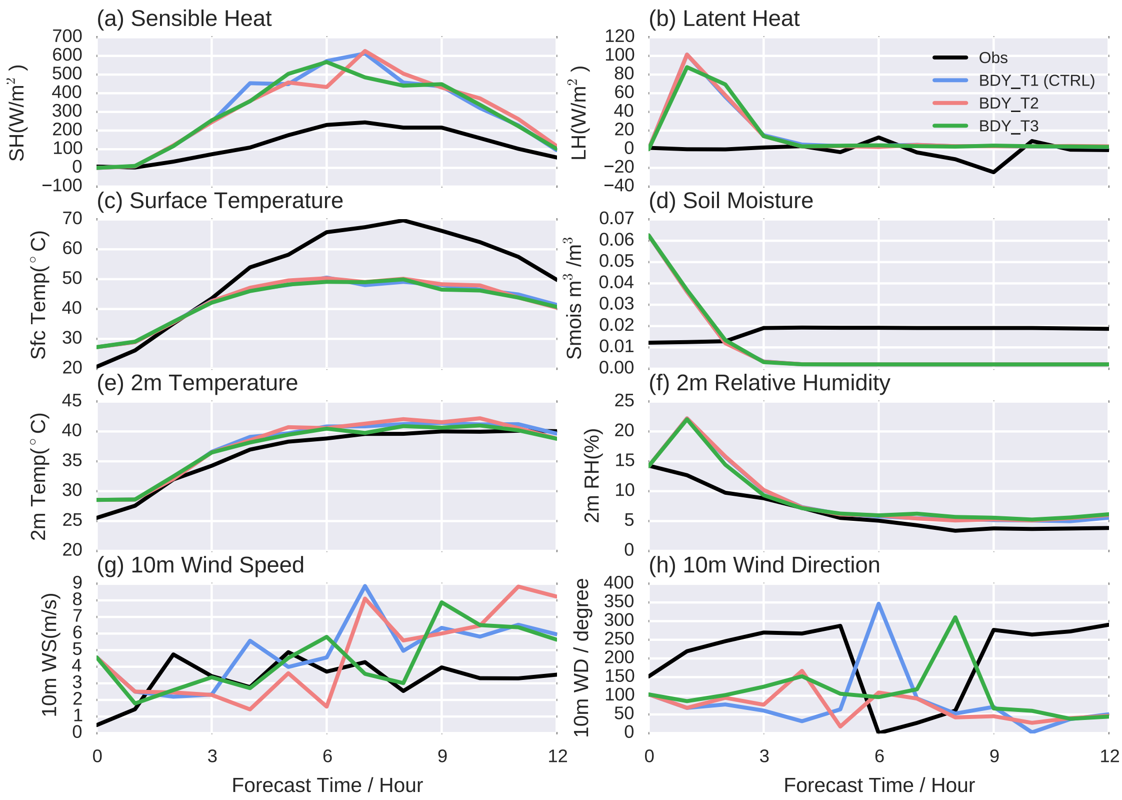

Figure 6 Time series of simulated surface initial at 0800 BJT 01July 2016 (a) sensible heat flux (W/m^2), (b) latent heat flux(W/m^2), (c) 2-m temperature (◦C), (d) surface temperature (◦C), (e) 2-m Relative Humidity(%) and (f) 10-m wind speed (m/s) with corresponding observations.

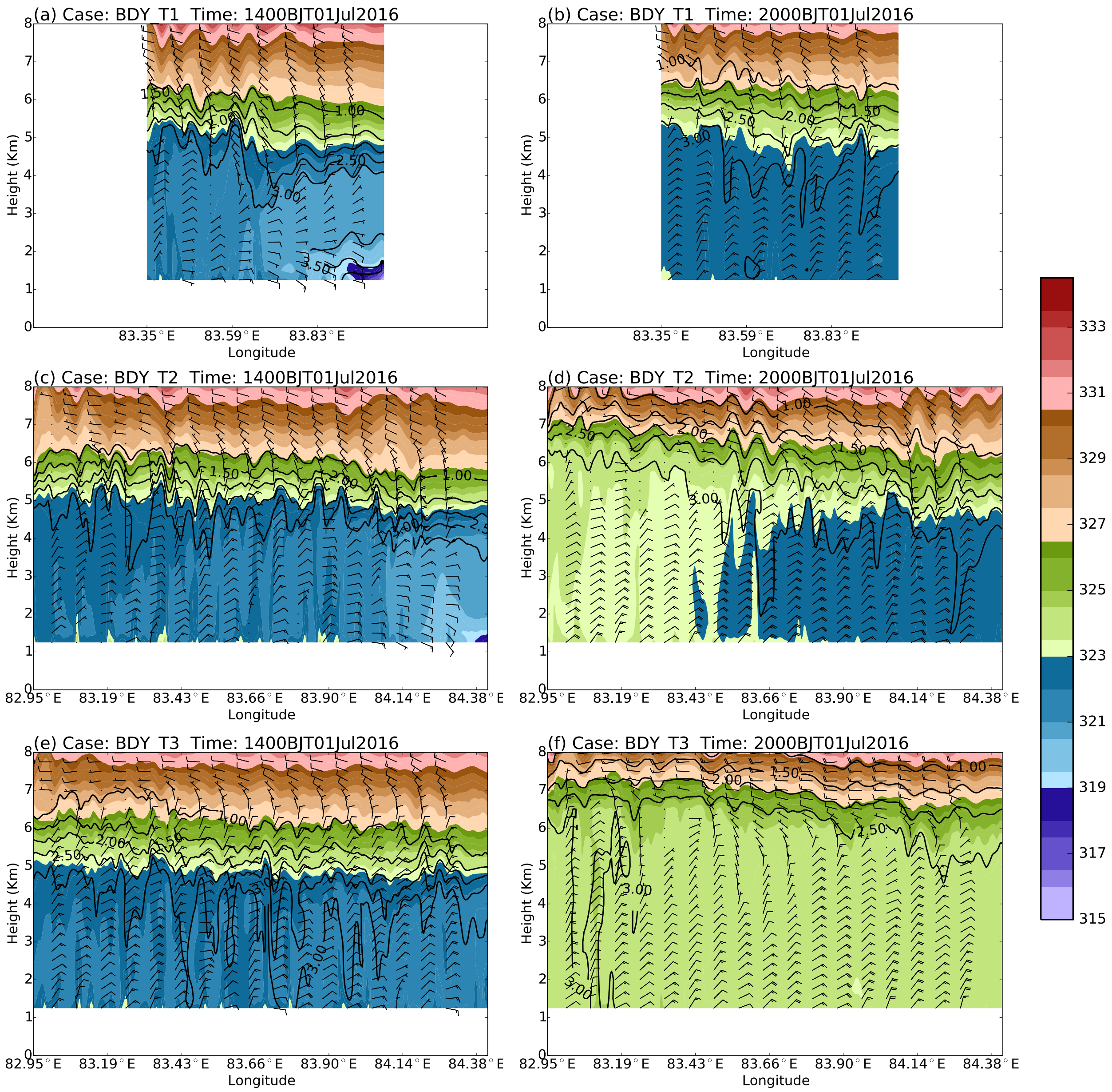

Figure 7 cross sections along 39.03°N of horizontal winds (barbs, units: m/s), at intervals of 5 m/s, superposed with theta (shaded, units: K) and vapor mixing ratio(contour, units: g/Kg), from (a) BDY_T1, (c) BDY_T2, (e) BDY_T3 experiments at1400 BJT 01JUL2016, (b), (d), (f) are the same as (a), (c), (e), but for 2000 BJT 01JUL2016.

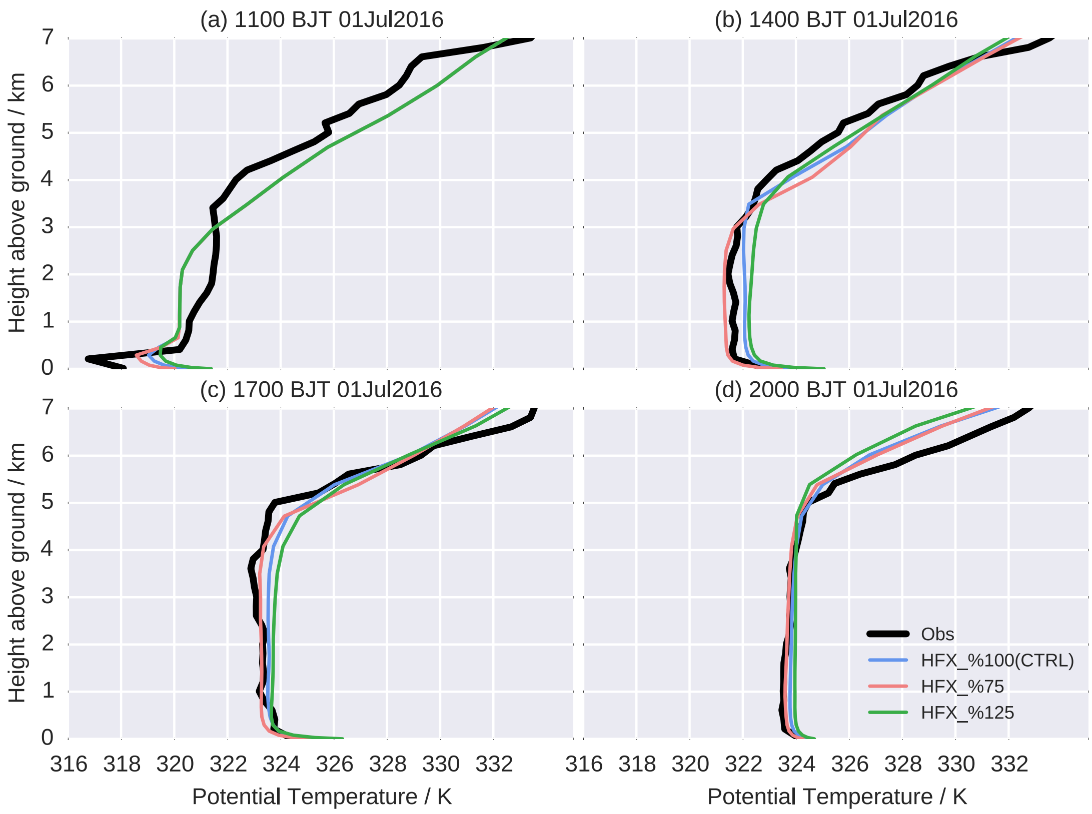

Figure 8 The same as Figure 4, but for SH flux sensitive experiment

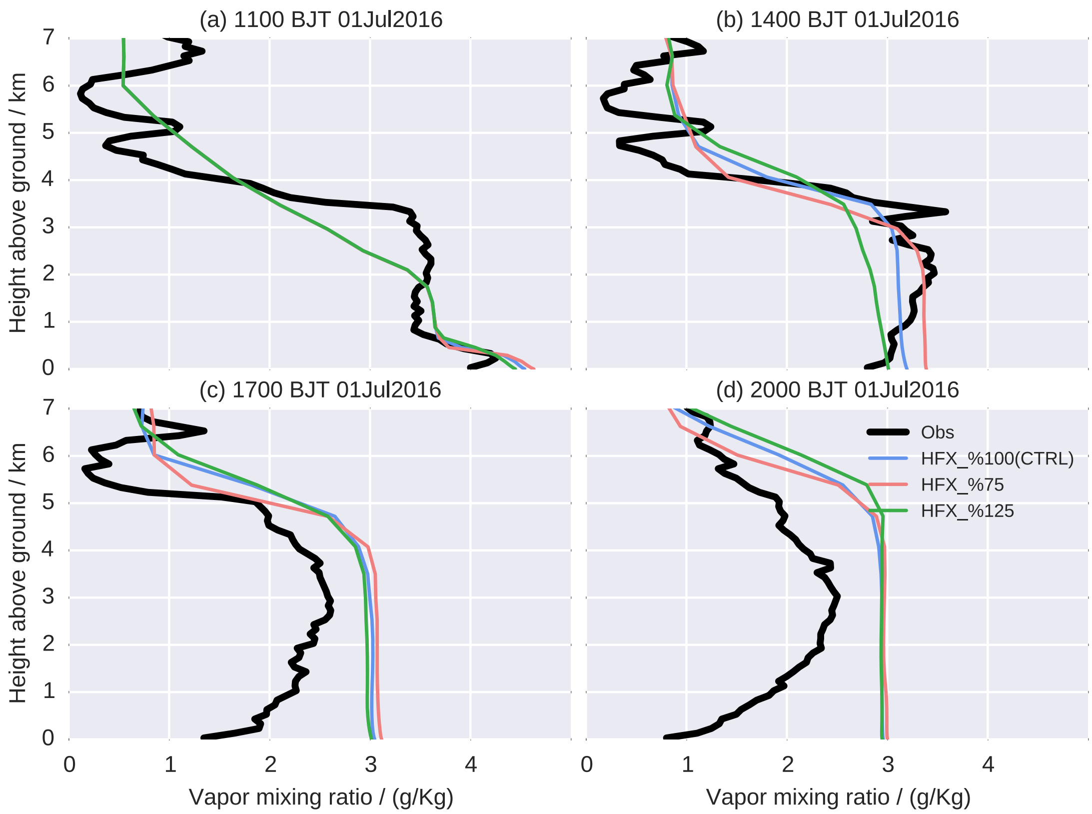

Figure 9 The same as Figure 8, but for vapor mixing ratio (units: g/Kg)

Experiment	Name	Remarks
1	BDY_T1(CTRL)	LBC of D04 is provide by d03 every 1 hour with model grids 403X406
2	BDY_T2	As BDY_T1, but LBC of D04 is provide by d03 every 6 hour
3	BDY_T3	As BDY_T2, but with model grids 205 X 208.

Table 1. List of designed experiments.

References

Chen, F., and J. Dudhia, 2001a: Coupling an advanced land surface-hydrology model with the Penn State-NCAR MM5 modeling system. Part I: Model implementation and sensitivity. *Monthly Weather Review*, **129,** 569-585.

——, 2001b: Coupling an Advanced Land Surface–Hydrology Model with the Penn State–NCAR MM5 Modeling System. Part II: Preliminary Model Validation. *Monthly Weather Review*, **129,** 587-604.

Dudhia, J., 1989: Numerical study of convection observed during the winter monsoon experiment using a mesoscale two-dimensional model. *J. Atmos. Sci.*, **46,** 3077-3107.

Engelstaedter, S., R. Washington, C. Flamant, D. J. Parker, C. J. T. Allen, and M. C. Todd, 2015: The Saharan heat low and moisture transport pathways in the central Sahara—Multiaircraft observations and Africa-LAM evaluation. *Journal of Geophysical Research: Atmospheres*, **120,** 2015JD023123.

Garcia-Carreras, L., and Coauthors, 2015: The Turbulent Structure and Diurnal Growth of the Saharan Atmospheric Boundary Layer. *Journal of the Atmospheric Sciences*, **72,** 693-713.

Heinold, B., P. Knippertz, and J. H. Marsham, 2013: Large Eddy Simulations of Nocturnal Low-Level Jets over Desert Regions and Implications for Dust Emission. *EGU General Assembly Conference*.

Heinold, B., P. Knippertz, and R. J. Beare, 2015: Idealized large-eddy simulations of nocturnal low-level jets over subtropical desert regions and implications for dust-generating winds. *Quarterly Journal of the Royal Meteorological Society*, **141,** 1740–1752.

Heinze, R., D. Mironov, and S. Raasch, 2015: Second-moment budgets in cloud topped boundary layers: A large-eddy simulation study. *Journal of Advances in Modeling Earth Systems*, **7,** 510-536.

Hong, S.-Y., and H.-L. Pan, 1996: Nonlocal boundary layer vertical diffusion in a medium-range forecast model. *Monthly weather review*, **124,** 2322-2339.

Hong, S.-Y., and J.-O. J. Lim, 2006: The WRF single-moment 6-class microphysics scheme (WSM6). *J. Korean Meteor. Soc*, **42,** 129-151.

Kain, J. S., 1993: Convective parameterization for mesoscale models: The Kain-Fritsch scheme. *The representation of cumulus convection in numerical models, Meteor. Monogr*, **46,** 165-170.

Kain, J. S., 2004: The Kain–Fritsch Convective Parameterization: An Update. *JOURNAL OF APPLIED METEOROLOGY*, **43,** 170-181.

LeMone, M. A., M. Tewari, F. Chen, and J. Dudhia, 2013: Objectively Determined Fair-Weather CBL Depths in the ARW-WRF Model and Their Comparison to CASES-97 Observations. *Monthly Weather Review*, **141,** 30-54.

Liu, Y., Q. He, H. Zhang, and A. Mamtimin, 2012: Improving the CoLM in Taklimakan Desert hinterland with accurate key parameters and an appropriate parameterization scheme. *Adv. Atmos. Sci.*, **29,** 381-390.

Liu, Y., and Coauthors, 2011: Simultaneous nested modeling from the synoptic scale to the LES scale for wind energy applications. *Journal of Wind Engineering and Industrial Aerodynamics*, **99,** 308-319.

Marsham, J. H., P. Knippertz, N. Dixon, D. J. Parker, and G. M. S. Lister, 2011: The importance of the representation of deep convection for modeled dust - generating winds over West Africa during summer. *Geophysical Research Letters*, **38.**

Mlawer, E. J., S. J. Taubman, P. D. Brown, M. J. Iacono, and S. A. Clough, 1997: Radiative transfer for inhomogeneous atmospheres: RRTM, a validated correlated-k model for the longwave. *J. Geophys. Res.*, **102,** 16663-16682.

Moeng, C.-H., J. Dudhia, J. Klemp, and P. Sullivan, 2007: Examining Two-Way Grid Nesting for Large Eddy Simulation of the PBL Using the WRF Model. *Monthly Weather Review*, **135,** 2295-2311.

National Centers for Environmental Prediction, N. W. S. N. U. S. D. o. C., 2015: NCEP GDAS/FNL 0.25 Degree Global Tropospheric Analyses and Forecast Grids. Research Data Archive at the National Center for Atmospheric Research, Computational and Information Systems Laboratory.

Schicker, I., D. Arnold Arias, and P. Seibert, 2016: Influences of updated land-use datasets on WRF simulations for two Austrian regions. *Meteorology and Atmospheric Physics*, **128,** 279-301.

Shin, H. H., and S. Y. Hong, 2011: Intercomparison of Planetary Boundary-Layer Parametrizations in the WRF Model for a Single Day from CASES-99. *Boundary-Layer Meteorology*, **139,** 261-281.

Shin, H. H., and S.-Y. Hong, 2015: Representation of the Subgrid-Scale Turbulent Transport in Convective Boundary Layers at Gray-Zone Resolutions. *Monthly Weather Review*, **143,** 250-271.

Skamarock, W. C., and Coauthors, 2008: A Description of the Advanced Research WRF Version 3. . *NCAR/TN–475+STR, NCAR TECHNICAL NOTE*.

Sun, J., and Q. Xu, 2009: Parameterization of Sheared Convective Entrainment in the First-Order Jump Model: Evaluation Through Large-Eddy Simulation. *Boundary-Layer Meteorology*, **132,** 279-288.

Talbot, C., E. Bou-Zeid, and J. Smith, 2012: Nested Mesoscale Large-Eddy Simulations with WRF: Performance in Real Test Cases. *Journal of Hydrometeorology*, **13,** 1421-1441.

ter Maat, H. W., E. J. Moors, R. W. A. Hutjes, A. A. M. Holtslag, and A. J. Dolman, 2012: Exploring the Impact of Land Cover and Topography on Rainfall Maxima in the Netherlands. *Journal of Hydrometeorology*, **14,** 524-542.

WANG, and Coauthors, 2016a: Summer atmospheric boundary layer structure in the hinterland of Taklimakan Desert, China. *Journal of Arid Land*, **8,** 846-860.

Wang, M. Z., H. Lu, H. Ming, and J. Zhang, 2016b: Vertical structure of summer clear-sky atmospheric boundary layer over the hinterland and southern margin of Taklamakan Desert: The deep convective boundary layer of Taklamakan Desert. *Meteorological Applications*, **23,** 438-447.